Real-time switching between multiple steady-states in quantum transport

A.-M. Uimonen[1], E. Khosravi[2,5,6], G. Stefanucci[3,5], S. Kurth[4,5], R. van Leeuwen[1,5], E.K.U. Gross[2,5,6]

[1]Department of Physics, Nanoscience Center, FIN 40014, University of Jyväskylä, Jyväskylä, Finland
[2]Institut für Theoretische Physik, Freie Universität Berlin, Arnimallee 14, 14195, Berlin, Germany
[3]Dipartimento di Fisica, Università di Roma Tor Vergata, Via della Ricerca Scientifica 1, I-00133 Rome, Italy
[4]Nano-Bio Spectroscopy Group, Dpto. de Física de Materiales, Universidad del País Vasco UPV/EHU, Centro Mixto CSIC-UPV/EHU, Av. Tolosa 72, E-20018 San Sebastián, Spain IKERBASQUE, Basque Foundation for Science, E-48011 Bilbao, Spain
[5]European Theoretical Spectroscopy Facility (ETSF)
[6]Max Planck Institute of Microstructure Physics, Weinberg 2, 06120, Halle, Germany

E-mail: anna-maija.uimonen@jyu.fi

Abstract. We study transport through an interacting model system consisting of a central correlated site coupled to finite bandwidth tight-binding leads, which are considered as effectively noninteracting. Its nonequilibrium properties are determined by real-time propagation of the Kadanoff-Baym equations after applying a bias voltage to the system. The electronic interactions on the central site are incorporated by means of self-energy approximations at Hartree-Fock, second Born and GW level. We investigate the conditions under which multiple steady-state solutions occur within different self-energy approximations, and analyze in detail the nature of these states from an analysis of their spectral functions. At the Hartree-Fock level at least two stable steady-state solutions with different densities and currents can be found. By applying a gate voltage-pulse at a given time we are able to switch between these solutions. With the same parameters we find only one steady-state solution when the self-consistent second Born and GW approximations are considered. We therefore conclude that treatment of many-body interactions beyond mean-field can destroy bistability and lead to qualitatively different results as compared those at mean-field level.

1. Introduction

The experimental observation [1, 2] of a hysteresis loop in the I/V characteristic of double-barrier resonant tunneling structures prompted intense theoretical activities to gain a microscopic understanding of this phenomenon. Several authors have been able to reproduce the hysteresis behavior by treating the Coulomb interaction at a mean field level [3, 4, 5, 6]. Self-consistent calculations have revealed the presence of bistable solutions, one of the solution being characterized by a considerable accumulation of charge in the potential well. Subsequent experimental work on double-barrier resonant tunneling diodes has, however, demonstrated that hysteresis loops do not always occur [7]. The suppression of the intrinsic bistability has been attributed to exchange-correlation effects [8].

With the advent of molecular electronics [9] the study of intrinsic bistability in nanoscale devices has gained attention due to the possibility of developing, for example, molecular diodes. So far, most of the work has focused on the steady-state I/V curve of molecular junctions attached to metallic leads. Up to date calculations are performed within the one-particle scheme of time-independent density functional theory (DFT). At the Hartree level bistability was reported by Negre *et. al* for a double quantum dot structure [10].

The mechanism of bistability and the calculation of switching times between two different states are mostly unexplored and the question how correlations affect the bistability has received very scarce attention. The purpose of the present exploratory paper is twofold: to extend the analysis to the time-domain and to study the role of memory effects in a bistable interacting resonant level model (IRLM).

Two complementary theoretical approaches will be used for calculating the time-dependent current and density, namely Time-Dependent (TD) DFT and Many-Body Perturbation Theory (MBPT). TDDFT [11] provide an exact framework to account for correlation effects both in the leads and the central region [12]. Within TDDFT the basic quantities that are propagated in time are the one-particle orbitals which depend on only one time variable. This property renders the implementation computationally favorable [13]. Most approximations to the TDDFT potential, however, do not include memory effects and the exchange-correlation part is approximated by local or semi-local functionals of the density. The lack of more sophisticated approximations represents, at present, a major obstacle for an accurate first principle description of TD quantum transport through interacting regions. MBPT has the advantage over TDDFT of allowing for a systematic inclusion of relevant physical processes through a selection of Feynman diagrams. Thus, MBPT provides an important tool to proceed beyond the commonly used adiabatic approximations and to quantify the importance of memory effects through advanced approximations to the self-energy. We recently proposed [14, 15] a time dependent MBPT formulation of quantum transport, based on the real-time propagation of the Green function [16, 17, 18] for open and interacting systems. First the Dyson equation for the connected system is solved to self-consistency on the imaginary axis. After that the Green function is propagated with the Kadanoff-Baym equations using different level of conserving approximations. As the Green function depends on two time variables the implementation of the MBPT scheme is more demanding than that of the TDDFT scheme. We expect that the interplay between MBPT and TDDFT will be essential to develop accurate approximation for systems more complex than the one studied here.

2. Interacting Resonant Level Model

We study an Anderson-type of system [19] where the impurity is an interacting site coupled to the infinite one dimensional tight-binding leads of finite band width. The Hamiltonian of the system reads

$$\begin{aligned}\hat{H}(t) &= \sum_{\sigma}[\varepsilon_0 + V_g(t)]\hat{d}^{\dagger}_{0\,\sigma}\hat{d}_{0,\sigma} + \frac{1}{2}\sum_{\sigma,\sigma'}\mathcal{U}\,\hat{d}^{\dagger}_{0,\sigma}\hat{d}^{\dagger}_{0,\sigma'}\hat{d}_{0,\sigma'}\hat{d}_{0,\sigma} + \sum_{i,\alpha,\sigma}[a + U_{\alpha}(t)]\hat{c}^{\dagger}_{i\alpha,\sigma}\hat{c}_{i\alpha,\sigma} \\ &+ \sum_{i,\alpha,\sigma}[b\hat{c}^{\dagger}_{i\alpha,\sigma}\hat{c}_{i+1\alpha,\sigma} + h.c.] + \sum_{\alpha,\sigma}[V_{0,1\alpha}\hat{d}^{\dagger}_{0,\sigma}\hat{c}_{1\alpha,\sigma} + h.c.], \qquad (1)\end{aligned}$$

where i denotes the site indices and σ is the spin index, ε_0 is the on-site energy of the localized site, $\mathcal{U}$ is the strength of the two-particle interaction on the central site, b is the hopping parameter between lead sites, $U_{\alpha}(t)$ is time-dependent bias voltage in the leads ($\alpha = L/R$), a is the on-site parameter in the leads and $V_{0,1\alpha}$ denotes coupling between the lead and the localized site. The fermionic creation- and annihilation operators in the leads α are denoted

as $\hat{c}^\dagger$, $\hat{c}$ whereas for the localized site they are denoted as $\hat{d}^\dagger$, $\hat{d}$. The quantity $V_g(t)$ denotes a time-dependent gate voltage.

The main reason for studying the IRLM is that for this system the multiple steady-state solutions are easily found from a fixed-point equation for the density on the localized site. The IRLM is the simplest system in which bistability occurs and hence allows for a clear interpretation of its multiple steady-state solutions. We study the system at a finite temperature and under a finite bias, such that we are out of the Kondo regime in which the IRLM is often used.

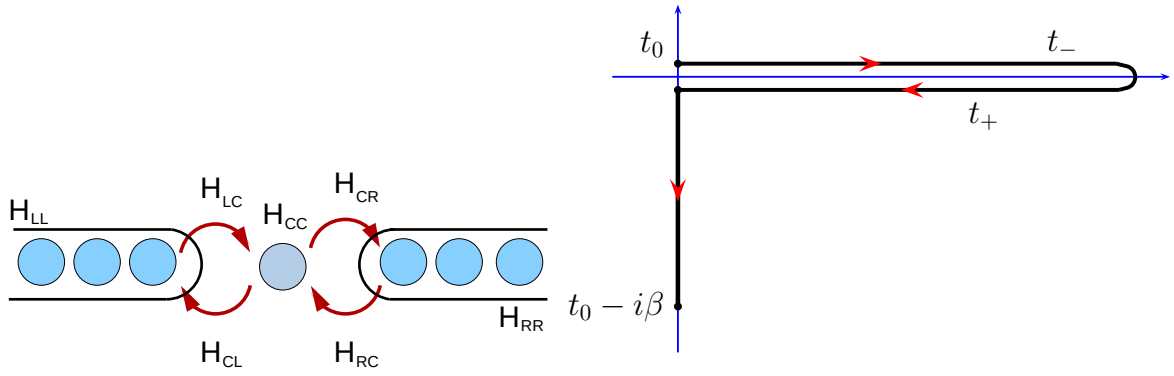

Figure 1: a) A schematic representation of the studied system. The correlated central region (C) is coupled to infinite one dimensional left (L) and right (R) tight-binding leads via a coupling Hamiltonian. b) The Keldysh contour c. Times on the lower branch t_+ are later than times on the upper branch t_-. The imaginary track extends up to the inverse temperature β.

3. Theoretical approach

3.1. Kadanoff-Baym equations

We study the nonequilibrium properties of the IRLM by means of time-propagation of the Kadanoff-Baym equations for the nonequilibrium Green function [20]. We assume the system to be contacted and in equilibrium at a chemical potential μ and at inverse temperature β before the time $t = t_0$. For $t > t_0$ the system is driven out of equilibrium by an external bias and we aim to study the time-evolution of the electron density and current. We give here a brief description of the approach described in more detail in Ref. [14].

The Keldysh Green function is defined as the expectation value of the contour ordered product [17]

$$G(1,2) = -i\frac{\mathrm{Tr}\{\hat{U}(t_0 - i\beta, t_0)\mathcal{T}_\mathcal{C}[\hat{\psi}_H(1)\hat{\psi}^\dagger_H(2)]\}}{\mathrm{Tr}\{\hat{U}(t_0 - i\beta, t_0)\}}, \tag{2}$$

where $\mathcal{T}_\mathcal{C}$ denotes the time ordering operator along the Keldysh contour c (see Fig.1b) and $\hat{U}$ is the time evolution operator. The average is taken over the grand canonical ensemble. We use the compact notation $1 = (\mathbf{x}_1, t_1)$ and $2 = (\mathbf{x}_2, t_2)$ where $\mathbf{x} = (\mathbf{r}, \sigma)$ is a collective space-spin index. From the Green function it is possible to calculate any one particle property of the system. For example the time-dependent density is given as

$$\langle \hat{n}(1) \rangle = -iG^<(1, 1^+), \tag{3}$$

where t^+ approaches t from an infinitesimally later time $t^+ = t + \delta$. The equation of motion for the full system can be derived from the definition of the Green function Eq. (2) and reads

$$[i\partial_{t_1} - H(1)]G(1,2) = \delta(1,2) + \int_c \mathrm{d}3\ \Sigma^{MB}[G](1,3)G(3,2), \tag{4}$$

where H is the one-body part of the Hamiltonian. The self-energy $\Sigma[G]$ incorporates all of the effects of exchange and correlation in the central region and is a functional of the Green function [17, 16]. In a localized basis the one-body part of the Hamiltonian (1) and the many-body self-energy can be written in a block-matrix form

$$H = \begin{pmatrix} H_{LL} & H_{LC} & 0 \\ H_{CL} & H_{CC} & H_{CR} \\ 0 & H_{RC} & H_{RR} \end{pmatrix}, \qquad \Sigma^{MB} = \begin{pmatrix} 0 & 0 & 0 \\ 0 & \Sigma^{MB}_{CC}[G_{CC}] & 0 \\ 0 & 0 & 0 \end{pmatrix}, \tag{5}$$

where the $H_{\alpha\alpha}$ and H_{CC} components describe the leads and the central system respectively, whereas the off-diagonal components describe the hopping between them [14]. We only consider the central region as interacting whereas the leads are effictively noninteracting. As a consequence, the many-body self-energy in Eq. (5) has non-vanishing elements only for the central region because the diagrammatic expansion starts and ends with an interaction line. In this work the electronic interactions are incorporated in $\Sigma^{MB}[G]$ at HF, 2B and GW level [14].

Solving the problem of an open infinite system is equivalent to solving the problem of a closed system with an equation of motion which considers the leads through an embedding term [14]. In our case this reads (in the reminder of this paper we will suppress the spatial indices of the objects involved)

$$[i\partial_t - H_{CC}(t)]\, G_{CC}(t,t') = \delta(t,t') + \int_c \mathrm{d}\bar{t}\ \left\{ \left[\Sigma_{em}(t,\bar{t}) + \Sigma^{MB}_{CC}[G_{CC}](t,\bar{t})\right] G_{CC}(\bar{t},t') \right\}, \tag{6}$$

where the embedding self-energy $\Sigma_{em}(t,t')$ accounts for the tunneling of electrons between leads and central region. In its general form, the embedding self-energy reads [14, 15, 21]

$$\Sigma_{em}(t,t') = \sum_\alpha \Sigma_{em,\alpha}(t,t') = \sum_\alpha H_{C\alpha} g_{\alpha\alpha}(t,t') H_{\alpha C}, \tag{7}$$

where $g_{\alpha\alpha}(t,t')$ is the lead Green function and $H_{C\alpha}, H_{\alpha C}$ is the coupling Hamiltonian between the central site and the leads.

The current through the lead α can be expressed in terms of Keldysh Green functions as [14, 15]

$$\begin{aligned} \mathrm{I}_\alpha(t) \quad &= \quad 2\mathrm{Re}\Big\{ \mathrm{Tr}_C \Big[\int_{t_0}^{t} d\bar{t} [G^<_{CC}(t,\bar{t})\Sigma^A_{em,\alpha}(\bar{t},t) + \int_{t_0}^{t} d\bar{t} G^R_{CC}(t,\bar{t})\Sigma^<_{em,\alpha}(\bar{t},t)] \\ &-i \quad \int_0^\beta d\bar{\tau} G^{\rceil}_{CC}(t,\bar{\tau})\Sigma^{\lceil}_{em,\alpha}(\bar{\tau},t) \Big] \Big\}, \end{aligned} \tag{8}$$

where we integrated on the Keldysh contour and where the superscripts $A, R, <$ refer to advanced/retarded/lesser component of Green function/self-energy and $\rceil, \lceil$ are the mixed components having one time argument on a imaginary axis and the other on the real axis [20, 18, 14]. The trace is taken over the central region. The current accounts for the initial many-body and embedding effects through the last term in equation (8) which is an integral

over the vertical track. Equation (8) is a generalization of the Meir-Wingreen formula [22]. We further define the nonequilibrium spectral function

$$A(T,\omega) = -\mathrm{Im}\,\mathrm{Tr}\int \frac{\mathrm{d}\tau}{2\pi} e^{i\omega\tau}[G^{>} - G^{<}](T+\frac{\tau}{2}, T-\frac{\tau}{2}), \tag{9}$$

where $\tau = t - t'$ is a relative time and $T = (t+t')/2$ is an average time coordinate. In equilibrium, this function is independent of T and has peaks below the Fermi level at the electron removal energies of the system, while above the Fermi level it has peaks at the electron addition energies. If the time-dependent external field becomes constant after some switching time, then also the spectral function becomes independent of T after some transient period and has peaks at the addition and removal energies of the biased system.

3.2. Time-dependent density functional theory

TDDFT provides an alternative framework to describe electron transport through interacting systems. In TDDFT [23] the time-dependent density of the interacting system is obtained through time-propagation of a Kohn-Sham system in an effective local potential. While in MBPT the correlation level is determined by the choice of the many-body self-energy, in TDDFT the main approximation is the functional used for the effective potential. The difficulty of TDDFT, compared to MBPT is the current lack of sufficient accurate approximations to the time-dependent exchange-correlation potential. However, the computational effort is much lower compared to a MBPT propagation.

The problem brought forward by considering an open system can be resolved in a very similar manner as in MBPT, with the help of an embedding self-energy. The equation of motion for the k-th single-particle orbital projected onto the central region, $\psi_{k,C}(t)$, reads

$$[i\partial_t - \mathrm{H}_{CC}(t)]\,\psi_{k,C}(t) = \int_0^t \mathrm{d}\bar{t}\,\Sigma^R_{em}(t,\bar{t})\psi_{k,C}(\bar{t}) + \sum_\alpha H_{C\alpha} g^R_{\alpha\alpha}(t,0)\psi_{k,\alpha}(0), \tag{10}$$

where $\Sigma^R_{em}(t,\bar{t})$ is the retarded embedding self-energy (see Eq. (7)) and $g^R_{\alpha\alpha}$ is the retarded lead Green function. The time-dependent density in the central region is obtained by

$$n(t) = \sum_k^{occ} |\psi_{k,C}(t)|^2, \tag{11}$$

where the summation is taken over all occupied orbitals in the time-dependent Slater determinant [24]. The technique to propagate Eq. (10) is described in detail in Ref. [13]. In this work we used this approach at a level, in which, for the system studied, the local exchange potential is equal to half the Hartree potential of the localized site. The results were found, as expected, to be identical to those obtained from the Kadanoff-Baym approach at HF level.

3.3. Steady-state density

We begin our study of the bistable regime by deriving an equation for the density on the localized site. This quantity is given by the lesser Green function at equal times

$$\langle \hat{n}(t) \rangle = -iG^{<}(t,t^+). \tag{12}$$

Since we consider the steady-state, we can assume that in the long-time limit the Green functions depend only on the relative time coordinate $t - t'$. In that case the Green function can be Fourier

transformed with respect to the relative time variable and the expression for the steady-state becomes

$$n = \int \frac{\mathrm{d}\omega}{2\pi i} G^{<}(\omega). \tag{13}$$

The Green function appearing in this expression satisfies the equation

$$G^{<}(\omega) = G^{R}(\omega)\Sigma^{<}_{tot}(\omega)G^{A}(\omega), \tag{14}$$

where $\Sigma^{<}_{tot}(\omega) = \Sigma^{<}_{em}(\omega) + \Sigma^{MB,<}_{CC}(\omega)$ and where $G^{A} = [G^{R}]^{*}$. The retarded Green function has the expression

$$G^{R}(\omega) = \left[\omega - \varepsilon_0 - \mathrm{Re}[\Sigma^{R}_{tot}(\omega)] - i\mathrm{Im}[\Sigma^{R}_{tot}(\omega)]\right]^{-1}. \tag{15}$$

For the tight-binding leads, that we consider, the retarded embedding self-energy is given by

$$\Sigma^{R}_{em,\alpha}(\omega) = \Lambda_\alpha(\omega) - \frac{i}{2}\Gamma_\alpha(\omega) = \frac{V_{1\alpha,0}V_{0,1\alpha}}{2b^2}\begin{cases} \omega_\alpha - \sqrt{\omega_\alpha^2 - 4b^2} & ,\omega_\alpha > 2|b| \\ \omega_\alpha + \sqrt{\omega_\alpha^2 - 4b^2} & ,\omega_\alpha < -2|b| \\ \omega_\alpha - i\sqrt{4b^2 - \omega_\alpha^2} & ,|\omega_\alpha| < 2|b| \end{cases} \tag{16}$$

where $\omega_\alpha = \omega - a + \mu - U_\alpha$, with the lead-on-site parameter a and the hopping parameter between the lead sites b. The chemical potential is denoted by μ, the applied bias for the lead α by U_α, and $V_{1\alpha,0}, V_{0,1\alpha}$ are the left/right couplings between leads and the central site. The lesser component of the embedding self-energy can be expressed as $\Sigma^{<}_{em,\alpha}(\omega) = i f_\alpha(\omega)\Gamma_\alpha(\omega)$ where f_α is the Fermi distribution of lead α and Γ_α is defined in Eq. (16).

If we integrate the left hand side of Eq. (14) over all frequencies then according to Eq. (13) we obtain an expression for the density per spin n on the localized site

$$n = \int_{-\infty}^{\infty} \frac{\mathrm{d}\omega}{2\pi} \frac{\Gamma_L(\omega)f_L(\omega) + \Gamma_R(\omega)f_R(\omega) - i\Sigma^{MB,<}_{CC}(\omega)}{(\omega - \mathrm{Re}[\Sigma^{MB,R}_{CC}(\omega)] - \Lambda(\omega))^2 + (\mathrm{Im}[\Sigma^{MB,R}_{CC}(\omega)] - \Gamma(\omega)/2)^2}, \tag{17}$$

where $\Lambda = \Lambda_R + \Lambda_L$ and $\Gamma = \Gamma_R + \Gamma_L$. This is a Meir-Wingreen-type equation for the density [25, 22] and is valid for transport through interacting systems. Within the HF approximation for the IRLM one has $\Sigma^{MB,<} = \mathrm{Im}[\Sigma^{MB,R}] = 0$ and $\mathrm{Re}[\Sigma^{MB,R}] = \mathcal{U}n$. Note that we include the time-singular part of the self-energy in the definition of the retarded/advanced component, see *e.g.*, [18]. Within this approximation, Eq. (17) now becomes a self-consistent fixed-point equation for the density n, since the value of the integral (17) depends on the density via the term $\mathcal{U}\,n$ in the denominator.

4. Results and discussion

We consider a biased system with the following parameters: $V_{0,1R} = V_{0,1L} = V = -0.35$, $\mathrm{U_L}$ = 1.5, $\mathrm{U_R}$ = 0.0, $\mathcal{U}$ = 2.0, b = -0.5, $a = \mu$ and μ = 0.3, β = 90. The leads are half-filled such that the Fermi level of lead α is positioned at $\mu + U_\alpha$ and the width of the lead band is $[\mu + U_\alpha - 2b, \mu + U_\alpha + 2b]$. With these parameters, within the HF approximation, the Meir-Wingreen approach [25, 22] predicts three solutions for the steady-state density n in Eq. (17). The three fixed points are shown in the inset of Fig. 2a, where we display the left and right hand side of Eq. (17). The corresponding densities are $n_1 = 0.33$, $n_2 = 0.58$ and $n_3 = 0.66$, which should be compared to the density of $n_0 = 0.28$ of the unbiased equilibrium state.

In 2a we show the steady-state spectral functions corresponding to these three solutions, which can be obtained directly from the retarded Green function $G^R(\omega)$. The peak of the spectral function corresponding to density $n_1 = 0.33$ is positioned at the energy 0.5. We thus see that this spectral function is located in an energy range within the right lead energy-band

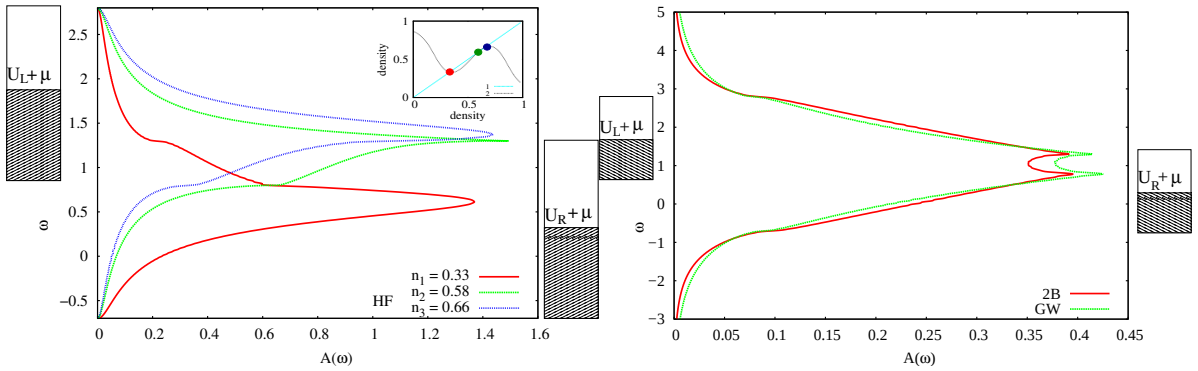

(a) (b)

Figure 2: a) Spectral functions for the HF approximation corresponding to different steady-state solutions. *Inset*: The graphical solution of the integral in Eq. (17): (1) is the left hand side of the equation whereas (2) is the value of the integral on the right hand side with given density n. b) Steady-state spectral functions for the 2nd Born and GW approximations.

(see right side of Fig. 2a). The spectral function corresponding to density $n_3 = 0.66$ is peaked approximately at energy 1.5 and is located in an energy range within the left lead energy-band. The HF spectral function corresponding second solution with density ($n_2 = 0.58$) is peaked on the top edge of the right lead energy-band and located in between the spectral functions corresponding to the densities n_1 and n_3. By time-propagation (see below), we find that the two solutions corresponding to densities n_1 and n_3 lead to stable steady-states, *i.e*, states that are reachable by time-propagation after applying a bias. On the other hand, the state corresponding to density n_2 is unstable and cannot be reached by time-propagation. The spectral function corresponding to the state with density n_2 has a large overlap with the one of density n_3. This indicates that (for sufficiently slow gate switching, see below) during the time-propagation more charge will flow onto the central site resulting in a stable steady-state with density n_3. From the analysis of the spectral functions we thus conclude that the density bistability in this system occurs when the spectral functions of the two stable solutions are localized well within one of the lead energy-bands and are well-separated. This happens exactly when the leads have a small overlap and the system is within the region of negative differential resistance (NDR).

Let us now consider the situation when we go beyond the HF approximation. In Fig. 2b we show the steady-state spectral functions for the 2B and GW approximations, as obtained from time-propagation of the Kadanoff-Baym equations. With these approximations we found only one steady-state solution, with very broad spectral function due to enhanced quasi-particle scattering at finite bias [14]. The spectral weight of the 2B and GW states is spread almost uniformly over the energy range from the bottom of the right lead energy band to the top of left lead energy band and extends well outside the lead bands. We also observe two small peaks in these spectral functions which occur approximately at 0.8 and 1.3, corresponding to the edges of the lead energy bands.

We now go to the time domain and consider how the steady-states at HF level, corresponding to densities $n_1 = 0.33$ and $n_3 = 0.66$, can be reached by time-propagation starting from the initially unbiased equilibrium state. We generate these steady-states by applying time-dependent gate pulses and we use the same technique to switch between them. In this work we have used

an exponentially decaying gate voltage of the form

$$V_g(t) = \begin{cases} V_g e^{-\gamma t} & , \text{ if } 0 < t < T_g \\ -V_g e^{-\gamma(t-T_g)} & , \text{ if } T_g < t < 2T_g \\ V_g e^{-\gamma(t-2T_g)} & , \text{ if } t > 2T_g \end{cases} . \tag{18}$$

The steady-state with density n_1 is obtained by time-propagation after applying a sudden constant bias $U_L(t) = U_L\theta(t)$ in the left lead, without applying the gate voltage. This is displayed in Fig. 3a. The steady-state of highest density n_3 is obtained (in addition to switching on the sudden bias in the leads) by applying an exponentially decaying gate voltage to the impurity site (with amplitude $V_g = 1.5$, decay rate $\gamma = 0.1$ and $T_g = \infty$).

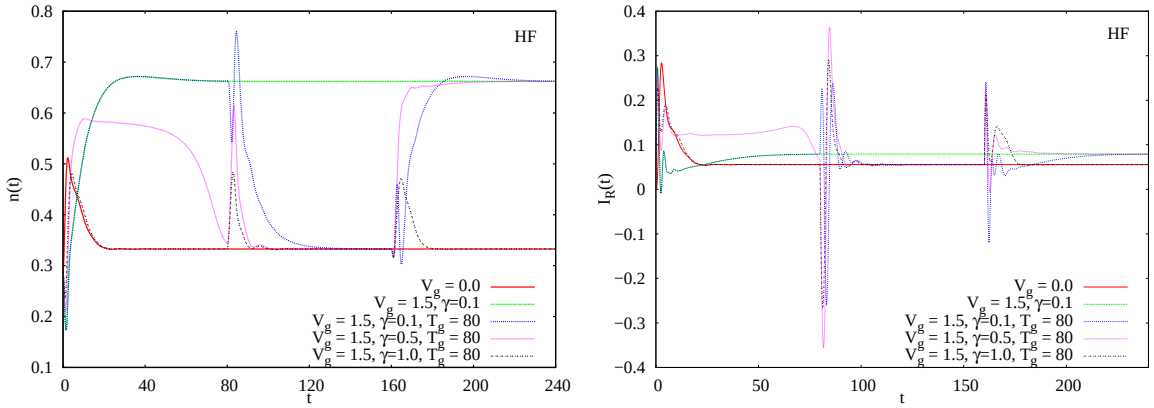

(a) (b)

Figure 3: a) Two different steady-state densities and the switching between the solutions by applying a gate voltage in the form of the equation (18). b) Two different steady-state currents through right lead and the switch between the solutions with a gate voltage of the form (18).

In Fig. 3a we show the time evolution of the density for various switchings between the steady-states. After we apply the first (sufficiently slow) gate voltage of equation (18) we let the system reach the steady-state of density n_3. At a time T_g we apply a second gate voltage in the opposite direction. The system shows a transient behavior after which, the system reaches the steady-state of density n_1. If we apply the third gate voltage at time $2T_g$ (see equation (18)), the system exhibits a short transient behavior and attains again the original steady-state of density n_3.

Corresponding to the densities n_1 and n_3 there are two distinguishable solutions for the currents $I_R(t)$ flowing into the right lead. These are shown in Fig. 3b where the lower value of the current corresponds to the state of density n_1 and the higher value of the current corresponds to the state of density n_3. The various transients observed in the density correspond directly to the transients in current shown in Fig. 3b. The frequency of the strongly damped oscillations of the transients (observed upon switching between the states in Fig.3b) is approximately given by the gate voltage, which causes a temporary change of V_g in the level position. As one can see from the Fig. 3a, if the decay rate $\gamma > 0.5$, *i.e.*, when the switching is too fast, the steady-state of density $n_3 = 0.66$ cannot be reached from the initial ground state of density $n_0 = 0.28$, because the system does not have enough time to acquire sufficient density.

In Fig. 4*a* we show, within the HF approximation, the nonequilibrium spectral function $A(T, \omega)$ of Eq.(9) for a switch (with $T_g = 60$, $V_g = 1.5$, and $\gamma = 0.1$) from the steady-state with

density n_1 to the state with density n_3. When the gate is applied, the upper side of the spectral peak, starts to oscillate. The spectral peak undergoes a transition and overshoots before it settles to a new value of 1.5 within the right lead band. During this transition we can observe the appearance of a sharp peak in the spectral function located approximately at energy 1.3 corresponding to the top edge of the right lead band. This is shown in the inset of Fig. 4a, where we display a snapshot of $A(T,\omega)$ at time $T = 70$ at which the central site has density $n(T) = 0.53$, which is very close to the density of unstable state n_2. Therefore, although this state does not lead to a steady-state, it can still be observed in the nonequilibrium spectral function.

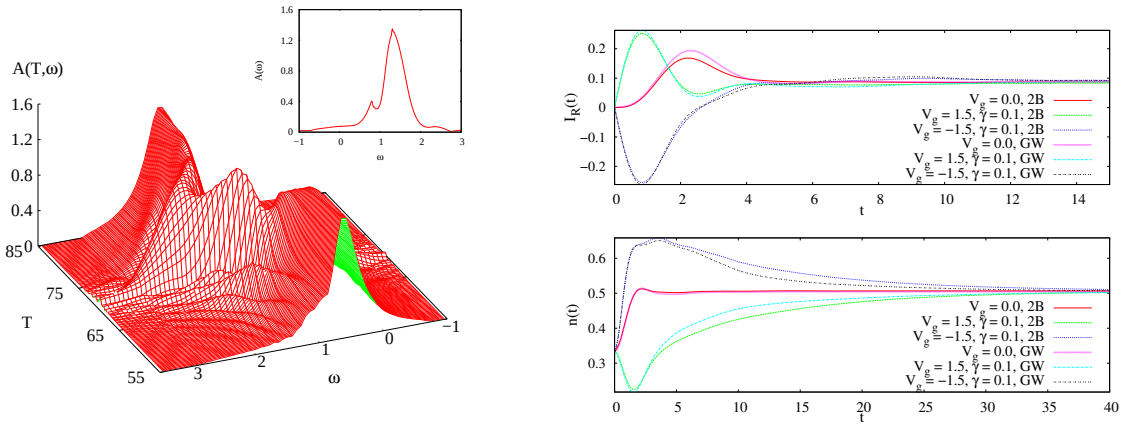

(a) (b)

Figure 4: a) Nonequilibrium spectral function $A(T,\omega)$ within the HF-approximation for the switch from the density n_1 to density n_3. *Inset*: Snapshot of spectral function corresponding to density n_2. b) The densities and currents calculated within the 2B and the GW approximations with and without an exponentially decaying gate voltage.

In Fig. 4b we show the densities and the currents obtained within the 2B and the GW self-energy approximations. For these cases only one steady-state is obtained with a density of about 0.5 on the central site. We have applied a time-dependent gate voltage of the form $V_g(t) = V_g e^{-\gamma t}$ for $t > 0$. If no gate is applied the transient regime is shorter and the density attains its steady-state value faster, compared to the case where the gate is applied. One can observe that the steady-state values of the currents and the densities for both GW and 2B are close to each other implying that for this system the single-bubble diagram, common to both approximations, plays a crucial role [14].

We conclude that for both the 2B and the GW approximation the spectral functions are very broad (see Fig. 2b) which makes it impossible to locate these spectral functions within an energy range in one of the lead energy-bands leading to two well-separated states. As a consequence the bistable regime is lost in the 2B and GW approximations, at least for the parameters considered.

5. Conclusions

In this paper we have investigated the switching between the steady-states of an interacting resonant level model connected to leads. For a given set of parameters we used a Meir-Wingreen type of approach to identify three different steady-state values for the density within the HF approximation. We showed that by applying an exponentially decaying gate voltage pulse during the time-propagation, at Hartree-Fock level, we can reach two different solutions and switch between them. However, due to a strong quasi-particle broadening of the spectral

function, bistability is lost when the second Born and GW approximations are considered. Hence treatment of many-body interactions beyond mean-field can destroy bistability and lead to qualitatively different results as compared to those at mean-field level.

References

[1] V. J. Goldman and D. C. Tsui. *Phys. Rev. Lett.*, 58(12), 1987.
[2] F. W. Sheard and G. A. Toombs. *Appl. Phys. Lett.*, 52(15), 1988.
[3] J. O. Sofo and A. Balsero. *Phys. Rev. B*, 42(7292), 1990.
[4] T. Fiig and A. P. Jauho. *Surface Science*, 267(392), 1992.
[5] P. L. Pernas and F. Florens. *Phys. Rev. B*, 47(4779), 1993.
[6] N.C. Kluksdahl, A.M. Kriman, D.K. Ferry, and C. Ringhofer. *Phys.Rev.B*, 39(7720), 1989.
[7] L. Eaves, G. A. Toombs, F. W. Sheard, C. A. Payling, M. L Leadbeater, E. S. Alves, T. J. Foster, P. E. Simmonds, M. Henini, O. H. Hughes, J. C. Portal, G. Hill, and M. A. Pate. *Appl. Phys. Lett.*, 52(212), 1997.
[8] N. Zou, M. Willander, I. Linnerud, U. Hanke, K. A. Chao, and Y. M. Galperin. *Phys. Rev. B*, 49(2193), 1994.
[9] M. Di Ventra. *Electrical Transport in Nanoscale Systems.* Cambridge University Press, 2008.
[10] C. F. A. Negre, P. A. Gallay, and C. G. Sánchez. *Chem. Phys. Lett.*, 460:220–224, 2008.
[11] R. M. Dreizler and E. K. U Gross. *Density Functional Theory: An Approach to the Quantum Many-Body Problem.* Springer-Verlag, New York, 1990.
[12] G. Stefanucci and C.-O. Almbladh. *Phys. Rev. B*, 69(195328), 2004.
[13] S. Kurth, G. Stefanucci, C.-O. Almbladh, A. Rubio, and E. K. U. Gross. *Phys. Rev. B*, 72(035308), 2005.
[14] P. Myöhänen, A. Stan, R. van Leeuwen, and G. Stefanucci. *Phys. Rev. B*, (accepted), 2009.
[15] P. Myöhänen, A. Stan, G. Stefanucci, and R. van Leeuwen. *Europhys. Lett.*, 84(67001), 2008.
[16] L. P. Kadanoff and G. Baym. *Quantum Statistical Mechanics.* Benjamin, New York, 1962.
[17] P. Danielewicz. *Ann. Phys. (NY)*, 152(239), 1984.
[18] N. E. Dahlen and R. van Leeuwen. *Phys. Rev. Lett.*, 98(153004), 2007.
[19] P. W. Anderson. *Phys. Rev.*, 124(1):41–53, 1961.
[20] R. van Leeuwen, N. E. Dahlen, G. Stefanucci, C.-O. Almbladh, and U. von Barth. Time-Dependent Density Functional Theory. *Lect. Notes Phys.*, 706:33–59, 2006.
[21] P. Myöhänen, A. Stan, R. van Leeuwen, and G. Stefanucci. Kadanoff-Baym approach to time-dependent quantum transport in AC and DC fields. *(these proceedings)*, 2009.
[22] Y. Meir and N. S. Wingreen. *Phys. Rev. Lett.*, 68(2512), 1992.
[23] M. A. L. Marques, C. A. Ullrich, F. Nogueira, A. Rubio, K. Burke, and E. K. U. Gross. *Time-Dependent Density Functional Theory.* Springer Heidelberg, 2006.
[24] A. Szabo and N. S. Ostlund. *Modern Quantum Chemistry: Introduction to Advanced Electronic Structure Theory.* Dover Publications, 1996.
[25] A. P. Jauho, N. S. Wingreen, and Y. Meir. *Phys. Rev. B*, 50(5528), 1994.
[26] A. L. Fetter and J. D. Walecka. *Quantum Theory of Many-Particle Systems.* Dover Publications, 1971.